

Liquid crystal droplets formation and stabilization during phase transition process

Xia Meng(孟霞), Jiayao Ye(叶家耀), Ao Li(李澳), Xudong Zhu(朱徐栋), Zhaoyan Yang(杨朝雁), Lei Wang(王磊), Bingxiang Li(李炳祥), and Yanqing Lu(陆延青)

Citation: Chin. Phys. B, 2024, 33 (**11**): 116101. DOI: 10.1088/1674-1056/ad7afd
Journal homepage: http://cpb.iphy.ac.cn; http://iopscience.iop.org/cpb

What follows is a list of articles you may be interested in

Stability of liquid crystal systems doped with γ-Fe_2O_3 nanoparticles

Xu Zhang(张旭), Ningning Liu(刘宁宁), Zongyuan Tang(唐宗元), Yingning Miao(缪应宁), Xiangshen Meng(孟祥申), Zhenghong He(何正红), Jian Li(李建), Minglei Cai(蔡明雷), Tongzhou Zhao(赵桐州), Changyong Yang(杨长勇), Hongyu Xing(邢红玉), and Wenjiang Ye(叶文江)
Chin. Phys. B, 2021, 30 (**9**): 096101. DOI: 10.1088/1674-1056/abeb11

Experimental design to measure the anchoring energy on substrate surface by using the alternating-current bridge

Hui-Ming Hao(郝慧明), Yao-Yao Liu(刘瑶瑶), Ping Zhang(张平), Ming-Lei Cai(蔡明雷), Xiao-Yan Wang(王晓燕), Ji-Liang Zhu(朱吉亮), Wen-Jiang Ye(叶文江)
Chin. Phys. B, 2017, 26 (**8**): 086102. DOI: 10.1088/1674-1056/26/8/086102

Thermo- and photo-driven soft actuators based on crosslinked liquid crystalline polymers

Wei Gu(顾伟), Jia Wei(韦嘉), Yanlei Yu(俞燕蕾)
Chin. Phys. B, 2016, 25 (**9**): 096103. DOI: 10.1088/1674-1056/25/9/096103

Azobenzene mesogens mediated preparation of SnS nanocrystals encapsulated with *in-situ* N-doped carbon and their enhanced electrochemical performance for lithium ion batteries application

Meng Wang(王勐), Yang Zhou(周旸), Junfei Duan(段军飞), Dongzhong Chen(谌东中)
Chin. Phys. B, 2016, 25 (**9**): 096102. DOI: 10.1088/1674-1056/25/9/096102

Phenomenological description of semi-soft nematic elastomers

Wen-Wen Diao(刁文文), Qing-Tian Meng(孟庆田), Fang-Fu Ye(叶方富)
Chin. Phys. B, 2016, 25 (**6**): 066103. DOI: 10.1088/1674-1056/25/6/066103

RAPID COMMUNICATION

Liquid crystal droplets formation and stabilization during phase transition process

Xia Meng(孟霞)[1], Jiayao Ye(叶家耀)[1], Ao Li(李澳)[1], Xudong Zhu(朱徐栋)[1], Zhaoyan Yang(杨朝雁)[1], Lei Wang(王磊)[1,2,†], Bingxiang Li(李炳祥)[1,‡], and Yanqing Lu(陆延青)[2]

[1] *College of Electronic and Optical Engineering & College of Flexible Electronics (Future Technology), Nanjing University of Posts and Telecommunications, Nanjing* 210023, *China*

[2] *National Laboratory of Solid State Microstructures, College of Engineering and Applied Sciences, Nanjing University, Nanjing* 210093, *China*

(Received 15 July 2024; revised manuscript received 18 August 2024; accepted manuscript online 14 September 2024)

The study of phase transition processes in liquid crystals (LCs) remains challenging. Most thermotropic LCs exhibit a narrow temperature range and a rapid phase transition from the isotropic (ISO) to the nematic (N) phase, which make it difficult to capture and manipulate the phase transition process. In this study, we observed the evolution of small droplets during the ISO–N phase transition in ferroelectric nematic (N_F) LC RM734. After doping with metal nanoparticles (NPs), the temperature range of the phase transition broadened, and the droplets formed during the phase transition remained stable, with their diameter increasing linearly with temperature. In addition, droplets doped with NPs can be well controlled by an external electric field. This discovery not only aids in understanding the fundamental mechanisms of LC phase transitions but also provides a simple alternative method for preparing droplets, which is potentially valuable for applications in optoelectronic devices and sensors.

Keywords: liquid crystal, droplets, phase transition process, metal nanoparticles

PACS: 61.30.−v, 61.30.Pq, 64.70.M–, 61.46.–w **DOI:** 10.1088/1674-1056/ad7afd

1. Introduction

Liquid crystals (LCs) exhibit an intermediate phase between liquids and solids, combining the fluidity of liquids with the orderliness of crystals. Their director distribution and optical properties strongly depend on the surface interactions and are highly sensitive to external stimuli, such as electric, magnetic, thermal, and light fields. These unique properties make them excellent tunable optoelectronic materials.[1] LCs play a significant role in multiple areas and have been widely applied in display technologies,[2] optoelectronic devices,[3] bioengineering,[4] etc. A particularly important aspect of LCs is their phase transition phenomenon, which involves transitions from one ordered or disordered state to another and encompasses complex physical mechanisms. Investigating these mechanisms not only provides fundamental insights into the nature of LCs but also paves the way for developing advanced materials and technologies.[5]

Typically, phase transitions are accompanied by nucleation and growth. The process is relatively fast, has a narrow temperature range, and is difficult to capture and control. Therefore, only a few researchers have investigated the spontaneous formation of droplets during the phase transition in thermotropic LCs. Golemme *et al.* studied continuous nematic (N)–isotropic (ISO) phase transition in submicron-sized LC droplets.[6] Schoot *et al.* theoretically examined the shape and director field of nematic liquid crystal (NLC) droplets and pointed out that the droplet formation is influenced by elastic energy and surface tension.[7,8] Sparavigna observed small droplets during the ISO–N phase transition of thermotropic LC 12OBAC using a polarizing optical microscope (POM) but did not provide a detailed analysis.[9] Nayani *et al.* investigated the droplets formed by lyotropic chromonic LCs during the phase transition from the ISO phase to an ordered amorphous phase, which can be used as optical probes to study the aggregation behavior of chromonics.[10] Wang *et al.* studied the spontaneous nucleation and transformation of cellulose nanocrystals from an ISO-phase dispersion to anisotropic LC droplets.[11] Li *et al.* found that aromatic rod-like LC oligomers/polymers could directly nucleate from the ISO phase to form ferroelectric nematic phase (N_F) droplets, exhibiting a phase transition process within a temperature range of less than 3 °C.[12] Overall, small droplets have been observed only for certain thermotropic LC materials.

In recent years, there has been extensive research on incorporating nanomaterials (NMs) ranging from zero dimension (0D) to two dimensions (2D) into LC systems[13–15] to regulate the physical properties of LCs. Sureshchandra *et al.* investigated the effect of nanoparticles (NPs) doping on the LC phase transition temperature and classified the resulting intermediate phases through texture analysis.[16] Kikuchi *et al.* also found that NLC composites doped with gold NPs achieved ISO and LC phases over a wide temperature range.[17] Ad-

†Corresponding author. E-mail: wangl@njupt.edu.cn
‡Corresponding author. E-mail: bxli@njupt.edu.cn

© 2024 Chinese Physical Society and IOP Publishing Ltd

ditionally, Melton *et al.* found that NPs can self-assemble and aggregate into defects in a confined environment of LC droplets.[18] These studies indicate that doped NPs significantly affect the phase transition temperature, phase state, and director field of LCs.

The N_F LCs exhibit transformative properties, including an ultrahigh dielectric constant, strong nonlinear optical response, low-voltage drive, and high fluidity.[19] They offer new possibilities for the development of innovative flexible optoelectronic devices. In 2020, Clark *et al.* first demonstrated that the LC material RM734 could form an N_F phase.[20] Since then, many researchers have extensively studied the relationship between the N_F phase of RM734 and its molecular structure, topological structure, and physical properties.[21–24] However, studies on the ISO–N phase transition of RM734 have often been overlooked. In this study, we focused on the ISO–N phase transition of RM734. Unlike the band texture phenomenon often observed during the N–N_F phase transition, the ISO–N phase transition proceeds through the spontaneous nucleation and growth of droplets. We first investigated the overall effect of temperature on the LC phase transition process, the basic mechanism of droplet formation, and then analyzed the growth process of individual droplets with temperature. We focused on the impact of doping metal NPs on the NLC droplets and realized that the LC droplets remained stable over a broad temperature range, and the performance of the electrically controlled droplets was improved.

2. Materials and methods

The LC cell is composed of two transparent glass substrates with inner surfaces coated with indium tin oxide (ITO). Both substrates were spin coated with polyimide (PI) (NC-M-4220, purchased from Nanjing Ningcui Optoelectronics Technology Co., Ltd., Nanjing, China) as the alignment layer, and the PI layers were rubbed for planar LC alignment. The substrates were bonded using a UV-curable adhesive mixed with spacers, and the cell thickness was controlled using spacers of different diameters. Metal NPs (Au @ Ag) with a diameter of 25 nm and RM734 were uniformly mixed in a volume ratio of 1:5. During the specific operation, we mixed 0.015 ml RM734 with 0.003 ml metal NPs and then mechanically stirred the mixture at 220 °C. Pure N_F LC RM734 and RM734 doped with NPs were separately added to cells above the clearing point temperature via capillary action. Stable LC droplets appeared during the ISO–N phase transition, as shown in Fig. 1.

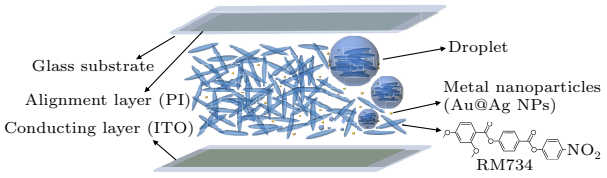


Fig. 1. Schematic of LC cell structure and NLC droplet formation during ISO–N phase transition. The inset shows the molecular structure of RM734.

3. Results and discussion

The cells filled with pure LC RM734 and the LC mixture doped with metal NPs were placed under a POM (CX40P series, purchased from Nanjing Jingcui Optoelectronics Technology Co., Ltd., Nanjing, China). Temperature was controlled during the heating stage. The LC was heated to the ISO phase, and cooled to observe the ISO–N–N_F phase transition process with cooling rate of 1 °C/min. The thickness of the LC cells was approximately 7 μm. As shown in Fig. 2, LC RM734 reached the ISO phase upon heating to 189 °C. During the cooling process, the phase transition occurred through droplet nucleation and growth, and the N phase formed fully at 186 °C, with the ISO–N phase transition process lasting for 3 °C. As cooling continued, a second phase transition started at 132 °C, marked by the strong destabilization of the uniform texture in the form of stripes. Gradually cooling further to 126 °C, the N_F phase formed, and periodic striped domains grew along the rubbing direction. The N–N_F phase transition process lasted for 6 °C. Upon further cooling to 70 °C, the LC did not crystallize.

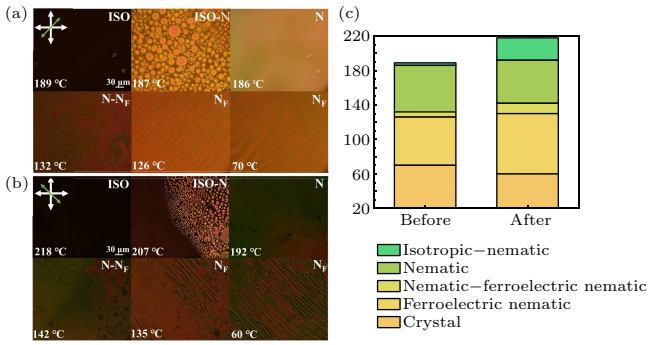


Fig. 2. ISO–N–N_F phase transition of RM734. (a) Texture of RM734 and (b) after doping with metal NPs. (c) Temperature ranges of each phase. Crossed bidirectional white arrows indicate the directions of the polarizer and analyzer, while the green arrow indicates the direction of the alignment.

After doping with metal NPs, the LC reached ISO phase when heated to 218 °C, and completely formed N phase when cooled to 192 °C. The ISO–N phase transition process lasted for about 26 °C. During this period, as the temperature decreased, small droplets appeared, which gradually increased in number and size. Upon further cooling to 142 °C, another phase transition occurred. When the sample was cooled slowly to 135 °C, a distinct N_F phase was observed. As the temperature continued to decrease, the domain area increased, and periodic stripe-like domains grew along the rubbing direction, alternating in an arrangement.[25] At 130 °C, the N_F phase was fully formed. The N–N_F phase transition spanned 12 °C. The sample did not crystallize upon further cooling to 60 °C.

Overall, the doped LC exhibited higher clearing point and phase transition temperature as well as a broader temperature range of phase transition than the undoped sample. This is likely due to the enhanced stability of the system resulting from the combination of metal NPs and LC molecules.[26–28]

During the cooling process from the ISO phase to the conventional N phase in the aforementioned two samples, circular droplet-like structures appeared. These droplets nucleated in the ISO phase, then grew and aggregated, evolving into an alignment layer dependent uniform N phase. Subsequently, we will focus on studying these often overlooked NLC droplets.

Typically, in the ISO phase, rod-like NLC molecules have centers and orientations in a disordered state. When the temperature decreases, the LC reaches a phase transition, in which the molecules uniformly turn their long axes in all spatial directions without moving their centers. The nucleus of the N phase initially grows in the ISO phase with spherical symmetry.[9] The total free energy density of the LC phase can be expressed as the sum of the phase transition free energy density f_{phase}, elastic free energy density f_{elastic}, and surface free energy density f_{surface}. Thus, the total free energy density f is expressed as[6,29,30]

$$f = f_{\text{phase}} + f_{\text{elastic}} + f_{\text{surface}}. \tag{1}$$

The phase transition free energy density f_{phase} can be expressed as

$$f_{\text{phase}} = \frac{1}{2}A_0(T - T_{\text{IN}})\text{tr}\boldsymbol{Q}^2 + \frac{1}{3}B\text{tr}\boldsymbol{Q}^3 + \frac{1}{4}C(\text{tr}\boldsymbol{Q}^2)^2, \tag{2}$$

where A_0, B, and C are the nematic material parameters, T is the temperature, and T_{IN} is the supercooling temperature. In this study, the N phase is oblate uniaxial (the usual rod-like N phase), hence $B < 0$. $C > 0$ ensures that the free energy density functional is bounded from below. $\boldsymbol{Q}$ is the third-order parameter tensor.

For uniaxial NLCs, the elastic free energy density f_{elastic} can be expressed as

$$\begin{aligned} f_{\text{elastic}} = \frac{1}{2}\big[&K_{11}(\nabla\cdot\boldsymbol{n})^2 + K_{22}(\boldsymbol{n}\cdot(\nabla\times\boldsymbol{n}))^2 \\ &+ K_{33}(\boldsymbol{n}\times(\nabla\times\boldsymbol{n}))^2\big], \end{aligned} \tag{3}$$

where $\boldsymbol{n}$ is the LC director. K_{11}, K_{22}, and K_{33} represent the elastic constants for splay, twist, and bend deformations, respectively. The elastic constants for RM734 are known:[31] K_{11}–2 PN, K_{22}–2.4 PN, and K_{33}–11.6 PN. Previous studies have shown that when $K_{33}/K_{11} > 1$, bipolar droplets are formed easily, and a larger ratio enhances the stability of the droplets.[32,33] We found that increasing K_{11} and K_{33} values led to the LC maintaining order at higher temperatures. K_{22} had a minor impact on the phase transition process. However, larger values of K_{22} slightly reduced the overall orderliness of the LC after the phase transition.

The surface free energy density f_{surface} can be expressed as

$$f_{\text{surface}} = \frac{1}{2}W(\tilde{\boldsymbol{Q}}_{ij} - \tilde{\boldsymbol{Q}}^{\perp}_{ij})^2, \tag{4}$$

where W denotes the anchoring strength coefficient. $\tilde{\boldsymbol{Q}}_{ij} = \boldsymbol{Q}_{ij} + S_{\text{eq}}\delta_{ij}/2$, $\tilde{\boldsymbol{Q}}^{\perp}_{ij} = P_{ik}\tilde{\boldsymbol{Q}}_{kl}P_{lj}$. S_{eq} is a uniaxial scalar-order parameter in the general bulk equilibrium state. $P_{ij} = \delta_{ij} - \upsilon_i\upsilon_j$ is the surface projection operator, δ_{ij} is the Kronecker delta function, and υ is the surface normal direction.

In this study, under the combined influence of the three free energies, RM734 can undergo the ISO–N phase transition process by nucleating, stabilizing growth, and aggregating into NLC droplets. During the phase transition, the system tends towards the state of minimum free energy. Upon reaching the phase transition temperature, the LC molecules gradually transition from disorder to order. Under the combined effects of elasticity and surface energy, droplets form, and with further temperature reduction, the droplets grow larger, merge with each other, eventually evolve into an alignment layer dependent uniform N phase. Experimental findings indicate that the temperature at which RM734 droplets doped with metal NPs reach ISO phase is higher and the temperature range of phase transition becomes wider. Moreover, the growth rate of droplets decreases, and they become more stable. This is believed to stem from the minimization of the droplet free energy due to the doped NPs.[27,34]

Using ImageJ (with a minimum detectable particle size of 20 pixels), we separately calculated the number of RM734 droplets and their phase area percentage before and after doping with metal NPs during the cooling process. Figures 3(a) and 3(b) depict the nucleation and growth processes of the droplets before and after doping with NPs, respectively. As shown, as the temperature decreased, the transition from none to multiple droplets occurred, followed by fusion. The curves in Figs. 3(c) and 3(d) show the variation in the droplet count and phase area percentage of the RM734 droplets with temperature. The droplet count gradually increased with decreasing temperature: peaking at 187.7 °C and, decreasing gradually, while the phase area percentage increased with decreasing temperature. Numerous small droplets emerged until approximately 187.6 °C, where the area change became gradual and slightly decreased with temperature. During this process, adjacent droplets gradually merged into larger droplets, resulting in a slightly smaller total area than the sum of the adjacent droplet areas, with a few new droplets forming. As the temperature dropped to approximately 187 °C, the droplet area steadily increased, with most droplets having completed one or more fusion events, stabilizing and accelerating fusion with neighboring droplets until all droplets merged to form the N phase. The temperature range for the phase transition was approximately 3 °C. Figures 3(e) and 3(f) illustrate the variation in the number of LC droplets and their phase area percentage during the cooling process after doping with metal NPs. During the phase transition, the droplet count increased with decreasing temperature, attained peak at approximately 203 °C, then decreased as adjacent droplets gradually merged until all transformed into the N phase. The phase-area per-

centage continuously increased over a wide temperature range. Compared to pure RM734, which exhibited fewer droplets and was less stable and prone to aggregation, the droplets after doping with NPs formed more stably during the phase transition process. NPs are believed to stabilize the phase structure during this period. They serve as nucleation points for specific LC phases, enhancing their stability and broadening the temperature range.[26,27] Next, we investigated the properties of individual droplets.

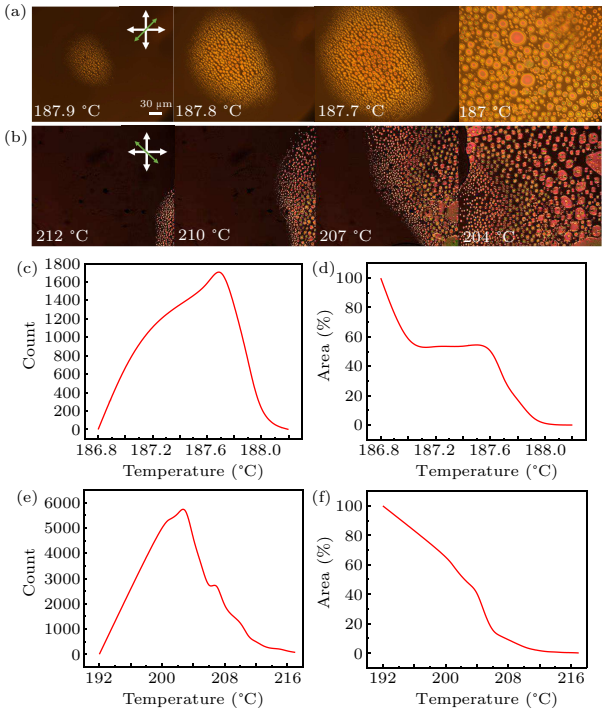


Fig. 3. Nucleation and growth process of droplets. (a) POM images of droplets formed by pure RM734 and (b) after doping with metal NPs. (c) Variation in count and (d) percentage of area of pure RM734 droplets during the cooling process. Temperature-dependent (e) variation in count and (f) percentage of area of metal NPs doped LC droplets.

Figure 4 illustrates the changes in single pure RM734 LC droplet and that doped with NPs during the cooling process. As shown in Figs. 4(a) and 4(b), with a slow decrease in temperature, the droplets gradually enlarged. We found that both before and after doping with NPs, the diameter of the LC droplets showed a linear relationship with temperature. Figure 4(c) shows that the droplet diameter increased linearly with temperature, with a slope of −34.64. Figure 4(d) demonstrates the temperature-dependent diameter changes of LC droplets doped with NPs, also exhibiting linear growth but with a gentler slope of −6.13, indicating increased stability due to NPs. The NPs stabilized the LC alignment, making it more resistant to change in temperature. Additionally, we observed distinct concentric circular patterns of color boundaries in LC droplets. Based on the above, it can be inferred that after doping with NPs, not only does the rate of droplet change slow down, but the texture also changes, indicating that the introduced NPs also affect the director field of the LC droplets.

Figure 5 shows the texture evolution of the two types of droplets as the microscope stage was rotated from 0° to 90°. Bipolar droplets were observed, as shown in Fig. 5(a), with darker centers and brighter edges, indicating that the LC director aligned along the tangential direction of the droplets. When the azimuthal angle of the bipolar axis (white line) was 0°, the LC director was parallel to the bottom polarizer in the large central region of the droplet and the texture appeared dark. In areas near the droplet boundary, the LC director was neither parallel nor perpendicular to the polarizer, resulting in a brighter appearance. As the azimuthal angle of the bipolar axis increased, the angle between the LC director and polarizer in the central region increased, making it brighter.[32,35] Figure 5(b) illustrates the texture evolution of the metal NP-doped LC droplets as they were rotated from 0° to 90°. The droplets still exhibited a bipolar configuration of the director field, but the internal color layering became more pronounced. Unlike undoped droplets, which showed increasing brightness at 30°, constant brightness at 60°, and decreasing brightness at 90°, droplets doped with NPs exhibited a significant increase in brightness at 30°. The texture changes in the droplets after doping with NPs indicate partial twist in the director field of the droplet,[36,37] as shown in Fig. 5(c). The NPs doped may lead to strong interactions with the LC molecules and stabilize the configuration of the droplets. These interactions influence the arrangement of LC molecules.[38,39]

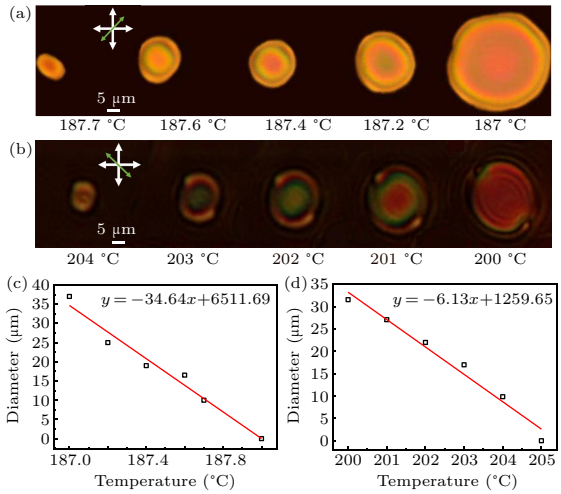


Fig. 4. Growth process of individual droplets. Microscopic images of the droplet (a) before and (b) after doping with NPs. Variation in droplet diameter before (c) and (d) after doping with NPs with temperature changes.

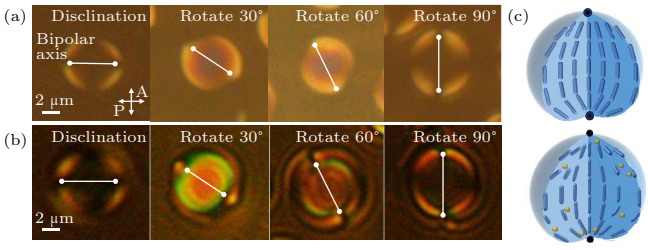


Fig. 5. Texture and director field of LC droplets at different azimuthal angles. (a) Optical texture of RM734 droplet and (b) after doping with metal NPs. Both samples exhibit typical bipolar director fields, with the bipolar axes located in the horizontal plane. (c) 3D diagrams illustrate the director fields.

A square-wave AC bias voltage of 1 kHz was applied to the top and bottom ITO substrates of the cell. Figure 6(a) illustrates the changes in the pure RM734 droplets formed before and after the application of an electric field. As the voltage gradually increased, reaching 1 V, the droplets that were already sensitive to external stimuli accelerated their transition to the N phase and merged with other droplets. Simultaneously, a color change was observed, indicating that the electric field altered the original alignment of the LC molecules. Figure 6(b) depicts the behavior of NP-doped droplets under different voltage conditions. The droplets remained stable, and as the voltage increased, the LC molecules inside the droplets gradually "stood up", indicating a gradual transition of the director vectors in a direction perpendicular to the cell substrate. Through POM, the transformation of the droplet texture and a gradual decrease in brightness were observed.

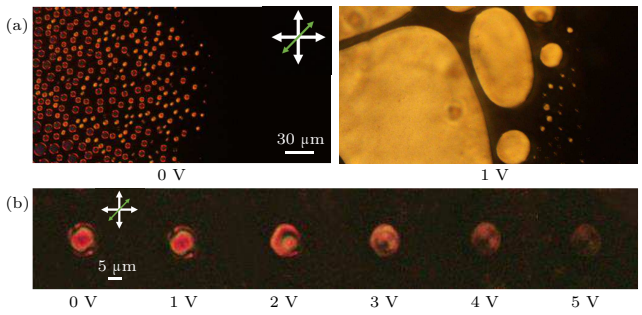


Fig. 6. Electrically tunable characteristics of LC droplets. (a) Changes in pure RM734 droplets before and after applying an electric field. (b) Changes in the droplets doped with metal NPs with different voltages.

LC droplets are currently widely used in various fields,[40] such as photonic communication,[41] functional material devices,[42–44] and sensing applications.[37,45] The droplets obtained using traditional mechanical stirring, oscillation, ultrasound, and other emulsification techniques have broad particle size distributions and difficult-to-control morphologies. Microfluidic technology provides an efficient and reliable approach for obtaining size- and structure-controllable LC droplets,[46] however, the preparation method is complicated. In this study, LC droplets spontaneously formed during the ISO–N phase transition process, and their configuration was further stabilized by metal NPs doping. External electric fields were applied to control the director field of the droplets. This type of droplets may have applications in temperature sensing, optical switching, and optical modulation.

4. Conclusion

In this study, we clearly observed the nucleation, growth, and aggregation of LC RM734 during the ISO–N phase transition process, occurring in the form of droplets. The interaction between the incorporated metal NPs and LC molecules expands the temperature range of phase transition, enabling the stable existence of droplets over a wider temperature range. The droplet diameter increases linearly within a certain range as the temperature decreases, and the external electric field can conveniently control the NLC droplets. This finding is beneficial for elucidating the fundamental mechanisms of LC phase transitions and droplet formation, provides a simple method for preparing droplets with specific functionalities, and holds potential application value in optoelectronic devices, biochemical sensing, and other fields.

Acknowledgments

Project supported by the National Key Research and Development Program of China (Grant No. 2022YFA1405000), the Natural Science Foundation of Jiangsu Province (Grant No. BK20211277), the Frontier Leading Technology Basic Research Project of Jiangsu Province (Grant No. BK20212004), the Postgraduate Research & Practice Innovation Program of Jiangsu Province (Grant No. KYCX23_0971), and the Natural Science Foundation of Nanjing University of Posts and Telecommunications (Grant No. NY223087).

References

[1] Maune H, Jost M, Reese R, Polat E, Nickel M and Jakoby R 2018 *Crystals* **8** 355
[2] Lu Y Q and Li Y 2021 *Light Sci. Appl.* **10** 122
[3] Kokhanchik P, Sigurdsson H, Piętka B, Szczytko J and Lagoudakis P G 2021 *Phys. Rev. B* **13** L081406
[4] Mahamid J, Tegunov D, Maiser A, Arnold J, Leonhardt H and Plitzko J M 2019 *Proc. Natl. Acad. Sci. USA* **116** 16866
[5] Singh S 2000 *Phys. Rep.* **324** 107
[6] Golemme A, Zumer S, Allender D W and Doane J W 1998 *Phys. Rev. Lett.* **61** 2937
[7] Prinsen P and Schoot P 2003 *Phys. Rev. E* **68** 21701
[8] Prinsen P and Schoot P 2004 *Eur. Phys. J. E* **13** 35
[9] Sparavigna A C 2016 *Philica* **1** 1208576
[10] Nayani K, Fu J, Chang R, Park J O and Srinivasarao M 2017 *Proc. Natl. Acad. Sci. USA* **114** 3826
[11] Wang P X and Maclachlan M J 2018 *Philos. Trans. A* **376** 20170042
[12] Li J, Xia R, Xu H, Yang J, Zhang X and Kougo J 2021 *J. Am. Chem. Soc.* **143** 17857
[13] Brouckaert N, Podoliak N, Orlova T, Bankova D, Fazio A F and Kanaras A G 2022 *Nanomaterials* **12** 341
[14] Ben Amor I, Saadaoui L, Alharbi A N, Althagafi T M and Soltani T 2022 *Chin. Phys. B* **31** 104202
[15] Xu Z, Liu N, Tang Z, Miao Y, Meng X, He Z, Li J, Cai M, Zhao T, Yang C, Xing H and Ye W 2021 *Chin. Phys. B* **30** 096101
[16] Sureshchandra J G, Prabhu P, Singh A, Sreeram B, Dhulia V and Yadav B S 2009 *Mol. Cryst. Liq. Cryst.* **511** 75
[17] Kikuchi H, Haseba Y, Yamamoto S I, Iwata T and Higuchi H 2009 *SID Symp. Dig. Tech. Papers* **40** 578
[18] Melton C N, Riahinasab S T, Keshavarz A, Stokes B J and Hirst L S 2018 *Nanomaterials* **8** 146
[19] Li J, Nishikawa H, Kougo J, Zhou J, Dai S and Tang W 2021 *Sci. Adv.* **7** 5047
[20] Chen X, Korblova E, Dong D, Wei X, Shao R and Radzihovsky L 2020 *Proc. Natl. Acad. Sci. USA* **117** 14021
[21] Ye F, Yang C, Zhang X, Huang X, Zhu Y and Aya S 2024 *J. Mater. Chem. C* **12** 2738
[22] Máthé M T, Himel M S H, Adaka A, Gleeson J T, Sprunt S and Salamon P 2024 *Adv. Funct. Mater.* **34** 2314158
[23] Yang J, Zou Y, Tang W, Li J, Huang M and Aya S 2022 *Nat. Commun.* **13** 7806
[24] Sebastian N, Lovsin M, Berteloot B, Osterman N, Petelin A and Mandle R J 2023 *Nat. Commun.* **14** 3029
[25] Mrukiewicz M, Perkowski P, Karcz J and Kula P 2023 *Phys. Chem. Chem. Phys.* **25** 13061

[26] Lalik S, Stefanczyk O, Dardas D, Gorska N, Ohkoshi S I and Marzec M 2021 *Materials* **14** 4722
[27] Draude A P, Kalavalapalli T Y, Iliut M, Mcconnell B and Dierking I 2020 *Nanoscale Adv.* **2** 2404
[28] Bukowczan A, Hebda E and Pielichowski K 2021 *J. Mol. Liq.* **321** 114849
[29] Erdmann J H, Žumer S and Doane J W 1990 *Phys. Rev. Lett.* **64** 1907
[30] Ravnik M and Žumer S 2009 *Liq. Cryst.* **36** 1201
[31] Mertelj A, Cmok L, Sebastián N, Mandle R J, Parker R R and Whitwood A C 2018 *Phys. Rev. X* **8** 041025
[32] Jiang J and Yang D K 2017 *Liq. Cryst.* **45** 102
[33] Ignés-Mullol J, Mora M, Martínez-Prat B, Vélez-Cerón I, Herrera R and Sagués F 2020 *Crystals* **10** 138
[34] Rahimi M, Roberts T F, Armas-Pérez J C, Wang W, Bukusoglu E and Abbott N L 2015 *Proc. Natl. Acad. Sci. USA* **112** 5297
[35] Yang C, Chen R, Feng L, Zhang R and Chen D 2022 *Soft Matter.* **2** 1022077
[36] Xu F and Crooker P P 1997 *Phys. Rev. E* **56** 6853
[37] Krakhalev M N, Prishchepa O O, Sutormin V S and Zyryanov V Y 2016 *Liq. Cryst.* **44** 355
[38] Lin I H, Miller D S, Bertics P J, Murphy C J, De Pablo J J and Abbott N L 2011 *Science* **332** 1297
[39] Prakash J, Khan S, Chauhan S and Biradar A M 2020 *J. Mol. Liq.* **297** 112052
[40] Yang C J and Chen D 2022 *Chin. J. Liq. Cryst. Disp.* **37** 1070
[41] Noh J, Liang H L, Drevenšek-Olenik I and Lagerwall J P F 2014 *J. Mater. Chem. C* **2** 806
[42] Miller D S, Wang X and Abbott N L 2014 *Chem. Mater.* **26** 496
[43] Lagerwall J P F and Scalia G 2012 *Curr. Appl. Phys.* **12** 1387
[44] Yang C J, Wu B H, Ruan J, Zhao P, Chen L, Chen D and Ye F F 2021 *Adv. Mater.* **33** 2006361
[45] Wang Y, Hu Q, Tian T and Yu L 2017 *Sens. Actuators B* **238** 676
[46] Schwartz M, Lenzini G, Geng Y, Ronne P B, Ryan P Y A and Lagerwall J P F 2018 *Adv. Mater.* **30** 1707382